

Human simulated intelligent control and its application in magneto-rheological suspension

DONG Xiao-min^{1,2}, LI Zu-shu³, YU Miao², LIAO Chang-rong², CHEN Wei-min²

(1. State Key Laboratory of Mechanical Transmission, Chongqing University, Chongqing 400044, China;

2. Key Lab of Optoelectronic Technology and System of Education Ministry, Chongqing University, Chongqing 400044, China;

3. Automatic College, Chongqing University, Chongqing 400044, China)

Abstract: The new advancement of human simulated intelligent control (HSIC) theory based on schema theory and its application in the magneto-rheological (MR) suspension system are studied. First, some fundamental concepts of HSIC based on sensory motor intelligent schema (SMIS) are defined by combing HSIC theory and schema theory. Then a general design principle of HSIC based on SMIS is given. Subsequently, on the basis of the general design principle, a human simulated intelligent controller based on SMIS is formulated for a MR suspension system with nonlinearity, time-delay and uncertainty. At last, the road test is performed to validate the proposed controller. The results have verified the universal validity of the HSIC theory based on SMIS to resolve complex system control problems.

Key words: human simulated intelligent control; schema theory; sensory motor intelligent schema; magneto-rheological suspension(MR)

CLC number: U463.33 **Document code:** A

仿人智能控制及其在磁流变半主动悬架中的应用

董小闵^{1,2}, 李祖枢³, 余 淼², 廖昌荣², 陈伟民²

(1. 重庆大学 机械传动国家重点实验室, 重庆 400044;

2. 重庆大学 光电技术及系统教育部重点实验室, 重庆 400044; 3. 重庆大学 自动化学院, 重庆 400044)

摘要: 论文讨论了基于图式理论的仿人智能控制理论最新进展及其在磁流变悬架中的应用情况. 首先, 结合图式理论和仿人智能控制理论, 定义一些基于动觉智能图式的仿人智能控制基本概念, 如感知图式、运动图式以及关联图式等. 然后, 给出了仿人智能控制器设计的通用性方法. 接着, 基于通用性的方法, 针对具有非线性、时滞及不确定性的磁流变悬架设计了基于动觉智能图式的仿人智能控制器. 最后, 开展了实车道路试验来验证控制方法的有效性. 试验结果表明, 基于动觉智能图式的仿人智能控制理论是解决复杂控制问题的有效途径.

关键词: 仿人智能控制; 图式理论; 动觉智能图式; 磁流变悬架

1 Introduction

In recent years, magneto-rheological(MR) dampers have received much attention for their rapid response to the applied magnetic field, compact size, insensitivity to temperature fluctuations, and low power requirements. They have demonstrated promise for automobile engineering in both analytical and experimental studies^[1]. However, one challenge in the use of MR technology is developing nonlinear control algorithms that are appropriate for implementation in suspension systems since the MR suspension system possesses sig-

nificant nonlinearity, time delay and uncertainty. Until now, various control algorithms, including simple linear feedback control algorithm, classic semi-active control strategies such as skyhook control, ground-hook control and hybrid control, modern control methods such as H-infinity^[2], and some intelligent control algorithms such as fuzzy logic control^[3] and neural network control^[4], have been tentatively applied in MR suspension to achieve better ride comfort and stability.

In our previous work^[2,5], the human simulated intelligent control(HSIC) based on the original algorithm

Received date: 2009-06-18; Revised date: 2009-11-19.

Foundation item: supported by the National Natural Science Foundation of China(60804018, 50830202); supported by the Post-doctoral Special Fund of People's Republic of China(200902292); supported by Chongqing Natural Science Foundation(CSTC.2008BB6184).

was proposed to apply in a half car suspension system with two MR dampers. The time delay and nonlinearity of the MR damper were studied. A modified simple feedback control strategy was adopted to linearize the nonlinear behavior of the MR damper; a Smith's predictor was formulated to compensate time delay of the control system. But the coupling relation between the pitch motion and the control inputs of the two MR dampers was not involved, which has significant effect on control performance of the MR suspension. Furthermore, the performance of the control algorithm was only validated by simulation and primary road test. As the continuation of our earlier work, the purpose of this study is to apply the improved HSIC based on sensory motor intelligent schema (SMIS) to a full vehicle MR suspension system and validate it through road test. To accomplish it, the theory and general design method of the improved HSIC based on SMIS is firstly analyzed. On the basis of the general design method, an HSIC controller based on SMIS is then formulated for full vehicle MR suspension system. Finally, the road test is performed to check the effectiveness of the proposed control strategy.

2 HSIC based on SMIS

The original human simulated intelligent control (HSIC) algorithm, which was firstly proposed by Prof. Zhou et al. in 1983^[6], has become a fundamental and systematic method used in resolving some general industrial control problems for the last twenties years. Nevertheless, the original theory has limitations in resolving some control objects with strong coupling, nonlinearity and high uncertainty such as two pendulums under limited torque or magneto-rheological semi-

active suspension system. To overcome the limitations of the original algorithm, the HSIC theory has been supplemented through combing with the schema theory of modern cognitive science in recent years. After having been studied for many years^[7], the HSIC theory based on SMIS has come into being. The theory provides a more effective and systematic method in resolving some complex control problems. A general design method and some fundamental concepts will be briefly addressed in the following.

From Fig.1, it can be concluded that a HSIC based on SMIS consists of sensed schema, associated schema and motion schema. In the following, the three schemas will be defined and addressed in turn.

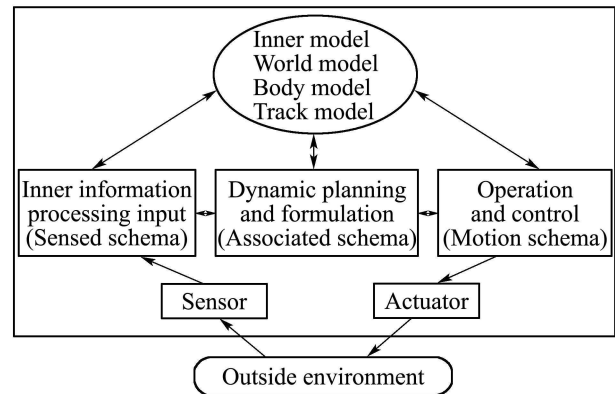


Fig. 1 Inner structure of HSIC base on SMIS

Definition 1(sensed schema) It is an intelligent module which can be formulated by an agent's repeatedly learning and accumulating control experiences. It has a structure as shown in Fig.2.

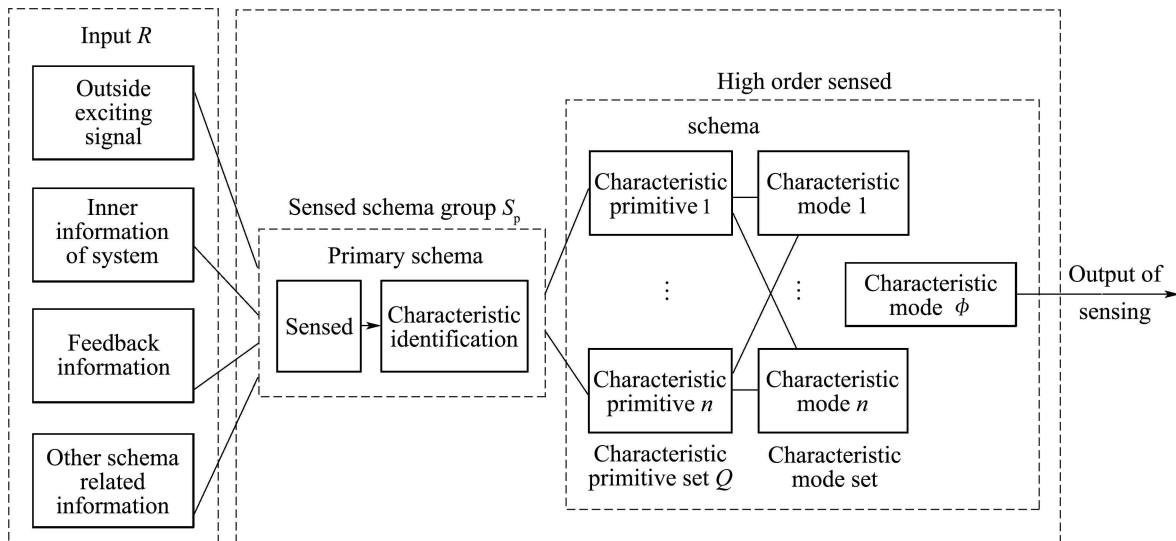


Fig. 2 Structure of sensed schema

A sensed schema group can be described in

$$S_p = \langle RQK \otimes \Phi \rangle. \quad (1)$$

In which:

$$\begin{aligned} R &= \{r_1, r_2, \dots, r_n\} \in \Sigma^n, \\ Q &= [q_1, q_2, \dots, q_m]^T \in \Sigma^m, K \in \Sigma^{r \times m}, \\ \Phi &= K \otimes Q = \\ \{\phi_1, \dots, \phi_i = K_i \otimes Q = \bigcap_{j=1}^m k_{ij} q_j \in \Sigma^q, \dots \\ \phi_q\} &\in \Sigma^r \end{aligned}$$

are the input information set, the characteristic prim-

itive set, the relation matrix, the operational symbol and the characteristic model set, respectively. The input information set can be one or more of the error of control input, the change of the error, peak value of the error etc. k_{ij} is an element of K and can be valued $-1, 0$ and 1 , which means taking negative, zeros and positive. Operational symbol is a “and” relation between two characteristic primitives.

Definition 2(motion schema) It is a stereotype embraced control strategy based on outside information of system and itself inner states. It has a structure shown in Fig. 3.

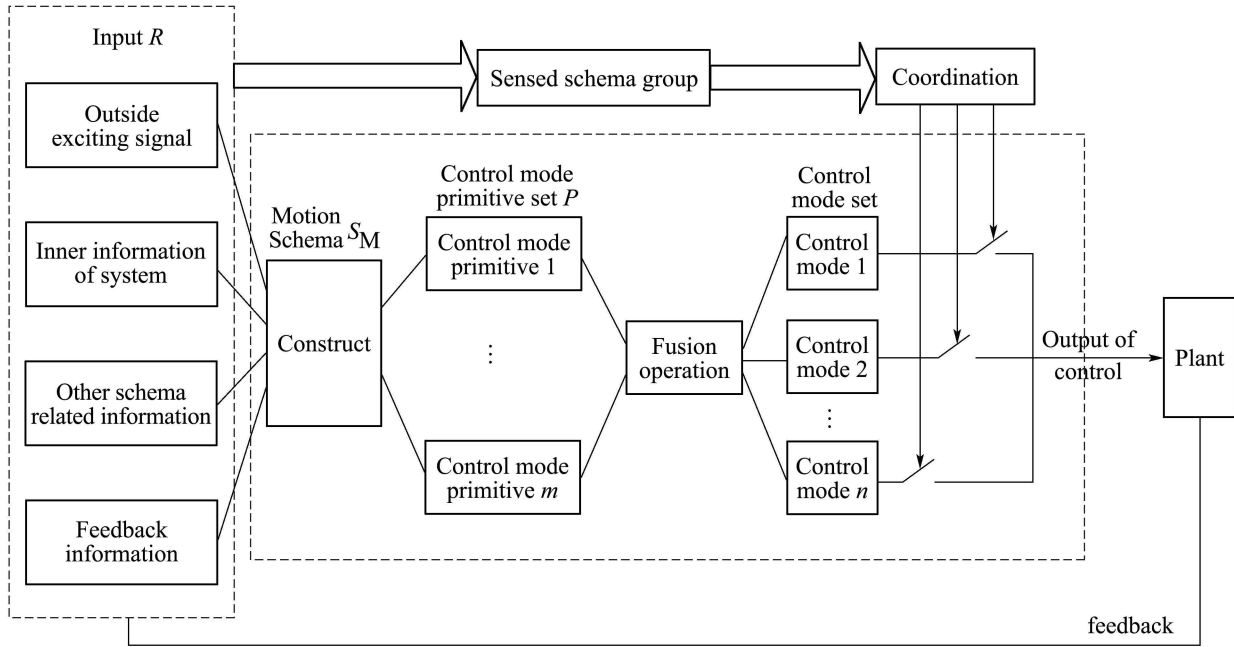


Fig. 3 Structure of motion schemas

A motion schema group can be formulated as

$$S_M = \langle RPL\Psi U \rangle. \quad (2)$$

In above,

$$\begin{aligned} R &\in \Sigma^d, \\ P &= [p_1, p_2, \dots, p_i = f(R), \dots, p_n]^T \in \Sigma^n, \\ L &\in \Sigma^{p \times n}, \\ \Psi &= \{\psi_1, \psi_2, \dots, \psi_i = L_i \cdot P = \\ \{u_i = \sum_{j=1}^n l_{ij} p_j\}, \dots, \psi_p\} &\in \Sigma^p, \end{aligned}$$

$U = L \cdot P$ are the input information set, the control mode primitive set, the coordination relation matrix, the control mode set and the control output, respectively. l_{ij} is an element of L and can be valued $-1, 0$

and 1 , which denote taking negative, zeros and positive, respectively. $P \in \Sigma^m$ is derived from some traditional control strategies, e.g. proportional control primitive $p_1 : k_p e$, differential control primitive $p_2 : k_d \dot{e}$, integral control primitive $p_3 : k_i \int e dt$, keeping control primitive $p_4 : k_h \sum_{i=1}^n e_{mi}$ etc. Control mode set $\Psi \in \Sigma^r$ is fused through combining mode primitive p_i , for example, a ‘proportional plus differential plus keeping’ control mode $\psi_1 : u_1 = u_H + k_p e + k_d \dot{e}$, an open loop control mode $\psi_2 : u = k \sum_{i=1}^n e_{mi}$ or a non-linear dead zone pre-compensation control mode $\psi_3 : u = u_n \pm a$.

Definition 3(associated schema) It is used to

coordinate the relation between the sensed schema and the motion schema, which simulates hu-

man's intuition reasoning and decision. It has a structure in Fig.4.

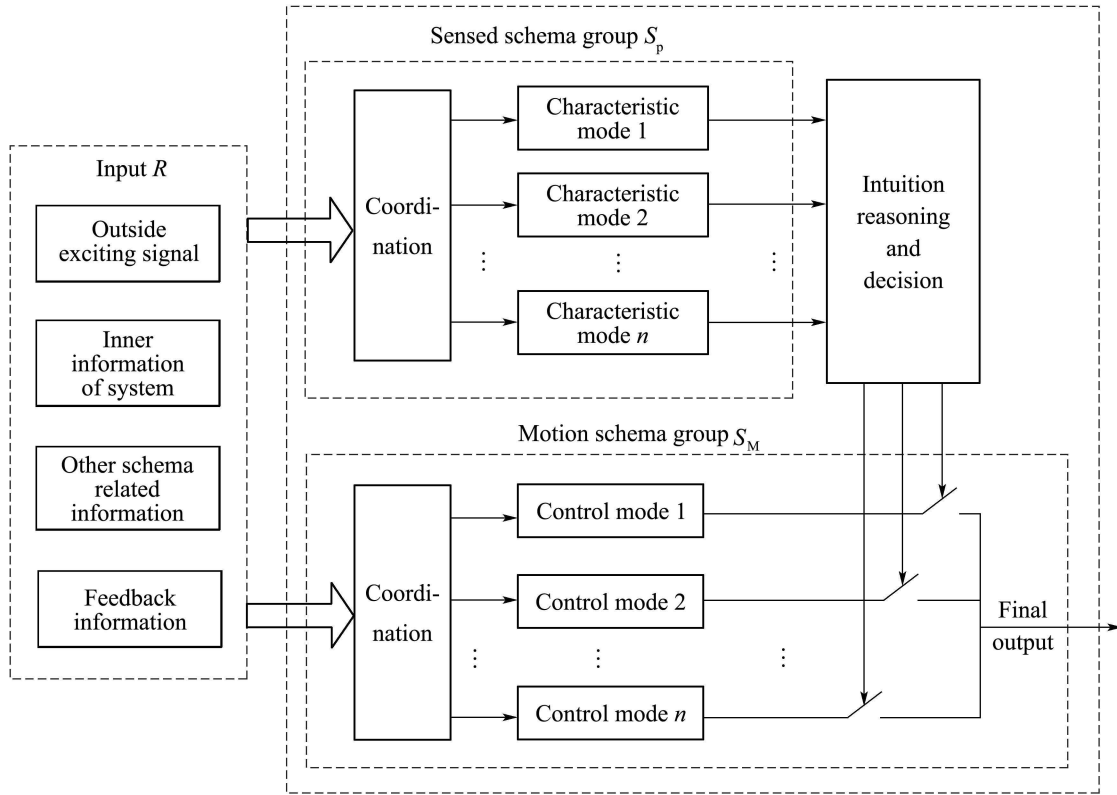


Fig. 4 Structure of associated schema

An associated schema can be written as

$$\Omega : \Phi \rightarrow \Psi, \Omega = \{w_1, w_2, w_3, \dots, w_r\},$$

$$\omega_i = \left\{ \text{if } \bigcup_j^{h_i(x)} \phi_{ij}, \text{ then } \psi_i \right\} \in \sum^r,$$

$$x \in q, h_i(x) = C_q^y, 1 \leq y \leq q.$$

in which x is the symbol of characteristic mode $\Phi_i (i = 1, 2, \dots, q)$, and $h_i(x)$ is a subset of characteristic mode symbols set $h_i(q)$, which has y elements.

After addressing the sensed schema, associated schema and motion schema of HSIC based on SMIS, a whole schema of HSIC, namely inner model can be described as

$$S_{KG} = \langle S_p, S_M, S_A \rangle, \quad (3)$$

where S_p, S_M, S_A are sensed schema, motion schema and associated schema, respectively.

3 HSIC controller for MR suspension system

3.1 Full vehicle dynamic model of MR suspension

A full car model with four MR dampers is shown in Fig.5. The car body itself is assumed to be rigid and has degrees of freedom in heave, pitch and roll directions. If state variables are defined as^[8]

$$x = [x_1, \dots, x_7]^T =$$

$$[z, \dot{z}, \theta, \dot{\theta}, \varphi, \dot{\varphi}, z_{ufl} - z_{rfl}, \dot{z}_{ufl},$$

$$z_{ufr} - z_{rfr}, \dot{z}_{ufr}, z_{url} - z_{rrl},$$

$$\dot{z}_{url}, z_{urr} - z_{rrr}, \dot{z}_{urr}]^T.$$

The state space form of the full vehicle MR suspension can be written as

$$\dot{x} = Ax + Bu + L\dot{w}. \quad (4)$$

where u is the control damping force of MR damper.

If considering the time-delay of MR suspension system, τ is time-delay. Then Eq.(4) can be written:

$$\dot{x} = Ax + Bu(t - \tau) + L\dot{w}. \quad (5)$$

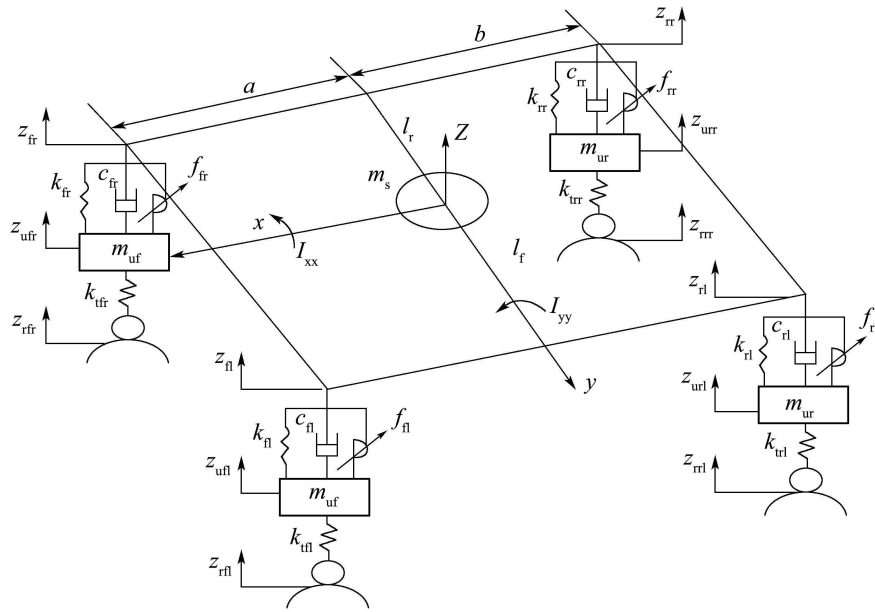


Fig. 5 Seven DOF for MR suspension

3.2 Control model of MR dampers

The MR damper in this work has the twin-tube structure that can operate with flow and shear modes, which is divided into the left and right chambers by the piston and is fully filled with the MR fluids.

This damping force of the MR damper can be continuously tuned by controlling the intensity of the magnetic field. The damping force of the MR damper can be given by Eq.(6) based on the Bingham fluid model, flowing in the parallel duct, which is composed of velocity damping force and Coulomb friction^[3].

$$F = -C_e V + F_{MR}. \quad (6)$$

in which: $C_e = \frac{24\eta A_p^2 l}{bh^3} + \frac{2\eta bl}{h}$, $F_{MR} = -(\frac{4lA_p}{\eta} + 2bl)\tau_y \text{sgn}(V)$, $b = 2\pi R_1$, A_p is the effective piston area, and equals the difference between the piston area and the piston rod area; R_1 is the inner radius of the cylinder; h is the width of damping path; l is the length of damping path; η is the viscosity of the MR fluid; and τ_y is the yield stress caused by the applied magnetic field or control current.

3.3 Development of HSIC controller

According to the general design methodology of HSIC theory addressed in Section 2, we can firstly regard a running car as a robot. A running car exhibits

one or more motions among heave, pitch, and roll motions for the sake of the disturbance of road and driver's maneuvers. It is difficult to suppress these vibrations with a single control model. Therefore, it is reasonable to apply multimode control strategy. Through much simulation and road test, it is feasible that motion attitudes of a running car are classified into nine types. These motion attitudes are the front-oriented pitch motion, the rear-oriented pitch motion, the left-oriented roll motion, the right-oriented roll motion, the heave motion, the front-oriented pitch motion plus heave motion, the rear-oriented pitch motion plus heave motion, the left-oriented roll motion plus heave motion and the right-oriented roll motion plus heave motion. For the first four motion attitudes, which are usually caused by the bump road or driver's emergency operation, their control aims is to improve the stability and some simple control strategies such as Bang-Bang are suitable. On the other hand, the other five motion attitudes, the control aims are to improve the ride comfort in that the driving stability can usually be assured. Hence, the control strategy can be chosen among Bang-Bang control, the skyhook control, the ground-hook control and the frequency-weighting. Since each SMIS of each motion attitude has the similar design procedure, only the SMIS of the first motion attitude is analyzed in detail. To deter-

mine the motion attitude of running car, characteristic set can be selected:

$$S_{P1} = (R_1, Q_1, K_1, \otimes, \Phi). \quad (7)$$

In which: $R_1 \in \Sigma^{14}$, $Q_1 \in \Sigma^9$, $K_1 \in \Sigma^{8 \times 9}$, $\Phi_1 \in \Sigma^8$. Characteristic primitive set is selected to effectively percept attitudes of running car and can be expressed as

$$Q_1 = \{q_1 ||z| \leq z_1, q_2 |\theta \dot{\theta} < 0, q_3 |\theta \dot{\theta} \geq 0, q_4 |\theta < -\theta_1, q_5 ||\varphi| < \varphi_1\}, \quad (8)$$

where z_1, θ_1, φ_1 are threshold values and can be adjusted during experiment.

The association matrix K_1 can be determined deflecting from or approaching the target attitude.

$$K_1 = \begin{Bmatrix} 1 & 1 & 0 & 1 & 1 \\ 1 & 0 & 1 & 1 & 1 \end{Bmatrix}.$$

As a result, the sensed characteristic model can be obtained.

$$\begin{cases} \Phi_1 = K_1 \otimes Q_1 = \{\phi_1 ||z| \leq z_1, \\ \theta \dot{\theta} < 0, \theta < -\theta_1, \\ |\varphi| \leq \varphi_1, \phi_2 ||z| \leq z_1, \\ \theta \dot{\theta} \geq 0, \theta < -\theta_1, |\varphi| \leq \varphi_1\}, \\ S_{M1} = (R_1, P_1, L_1, \Psi_1, U_1), \end{cases} \quad (9)$$

where, $P_1 \in \Sigma^8$, $L_1 \in \Sigma^{8 \times 8}$, $\Psi_1 \in \Sigma^8$.

When the front-oriented pitch motion is perceived, the control mode can be selected between Bang-Bang control and ground-hook control to improve driver's stability. Thus the primitive set of motion schema can be written as

$$P_1 = \{p_1 | u = U_1 = (u_{\max}, u_{\max}, 0, 0)^T, \\ p_2 | u = U_{\text{ground1}} = (c_{\text{ground}} \dot{z}_{\text{uff}}, c_{\text{ground}} \dot{z}_{\text{ufr}}, \\ c_{\text{ground}} \dot{z}_{\text{url}}, c_{\text{ground}} \dot{z}_{\text{urr}})^T\}.$$

The mode selection matrix is $L_1 = \begin{Bmatrix} 1 & 0 \\ 0 & 1 \end{Bmatrix}$.

For each SMIS, the control problem solving is in reality a combination of qualitative and quantitative double mapping information process and decision procedure:

$$S_{A1} = \{\Omega_1 : \phi_1 \rightarrow \psi_1\}.$$

After designing the sensed schema, the motion schema and the associated schema, the whole SMIS of the front-oriented pitch motion can be written in the following.

$$S_{KG1} = \begin{cases} u = U_1, \\ |z| \leq z_1, |\varphi| < \varphi_1, \theta < -\theta_1, \theta \dot{\theta} < 0, \\ u = U_{\text{ground1}}, \\ |z| \leq z_1, |\varphi| < \varphi_1, \theta < -\theta_1, \theta \dot{\theta} \geq 0. \end{cases} \quad (10)$$

Similar to the first motion attitude, the SMIS of the second to the ninth can also be designed and written as

$$S_{KG2} = \begin{cases} u = U_2, \\ |z| \leq z_1, |\varphi| < \varphi_1, \theta > \theta_1, \theta \dot{\theta} < 0, \\ u = U_{\text{ground2}}, \\ |z| \leq z_1, |\varphi| < \varphi_1, \theta > \theta_1, \theta \dot{\theta} \geq 0, \end{cases} \quad (11)$$

$$S_{KG3} = \begin{cases} u = U_3, \\ |z| \leq z_1, |\theta| < \theta_1, \varphi > -\varphi_1, \theta \dot{\theta} < 0, \\ u = U_{\text{ground3}}, \\ |z| \leq z_1, |\theta| < \theta_1, \varphi > -\varphi_1, \theta \dot{\theta} \geq 0, \end{cases} \quad (12)$$

$$S_{KG4} = \begin{cases} u = U_4, \\ |z| \leq z_1, |\theta| < \theta_1, \varphi > \varphi_1, \theta \dot{\theta} < 0, \\ u = U_{\text{ground4}}, \\ |z| \leq z_1, |\theta| < \theta_1, \varphi > \varphi_1, \theta \dot{\theta} \geq 0, \end{cases} \quad (13)$$

$$S_{KG5} = \begin{cases} u = U_{\text{sky5}}, \\ |\theta| < \theta_1, |\varphi| < \varphi_1, |z| > z_1, |z| \leq z_2, \\ u = U_{\text{wf5}}, \\ |\theta| < \theta_1, |\varphi| < \varphi_1, |z| > z_2, \end{cases} \quad (14)$$

$$S_{KG6} = \begin{cases} u = aU_1 + (1-a)U_{\text{sky5}}, \\ \theta < -\theta_1, |\varphi| < \varphi_1, |z| > z_1, |z| \leq z_2, \\ u = aU_{\text{ground1}} + (1-a)U_{\text{wf5}}, \\ \theta < -\theta_1 \& |\varphi| < \varphi_1 \& |z| > z_2, \end{cases} \quad (15)$$

$$S_{KG7} = \begin{cases} u = aU_2 + (1-a)U_{\text{sky5}}, \\ \theta > \theta_1, |\varphi| < \varphi_1, |z| > z_1, |z| \leq z_2, \\ u = aU_{\text{ground2}} + (1-a)U_{\text{wf5}}, \\ \theta > \theta_1, |\varphi| < \varphi_1, |z| > z_2, \end{cases} \quad (16)$$

$$S_{KG8} = \begin{cases} u = \beta U_3 + (1 - \beta)U_{sky5}, \\ \varphi < -\varphi_1, |\theta| < \theta_1, |z| > z_1, |z| \leq z_2, \\ u = \beta U_{ground3} + (1 - \beta)U_{wf5}, \\ \varphi < -\varphi_1, |\theta| < \theta_1, |z| > z_2, \end{cases} \quad (17)$$

$$S_{KG9} = \begin{cases} u = \beta U_4 + (1 - \beta)U_{sky5}, \\ \varphi > \varphi_1, |\theta| < \theta_1, |z| > z_1, |z| \leq z_2, \\ u = \beta U_{ground4} + (1 - \beta)U_{wf5}, \\ \varphi > \varphi_1, |\theta| < \theta_1, |z| > z_2, \end{cases} \quad (18)$$

where, $U_i(i = 1, \dots, 4)$, φ_1 , θ_1 , z_1 , z_2 are some threshold values, $U_{groundi}(i = 1, \dots, 4)$, U_{sky5} , U_{wf5} are control forces calculated by ground-hook, sky-hook and frequency-weighting control^[3], respectively, a, β are weighting factors and are between 0 and 1.

4 Road test and results

To validate the proposed control strategy, a middle-sized passenger car is selected as the test car. The passenger car has a total length of 4215 mm, total width of 1675 mm, total height of 1375 mm, wheelbase of 2610 mm, front track and rear track of 1470 mm and weight of 1020 kg. Four MR dampers are used to replace the passive ones of the test car. Simultaneously, the rapid control prototype(RCP) technology is adopted to reduce the time consumption of hardware development. The RCP technology based on dSPACE, which consists of DS1005 PPC board, DS2002 multi-Channel A/D Board and DS2102 high-resolution D/A Board, is fabricated in Fig.6. The dSPACE system is fastened in luggage boot and employed to control the four MR dampers respectively.



Fig. 6 Setup of the test car

Four accelerometers are placed on the vehicle body's four corners to record the vertical acceleration signal of the sprung mass, and four are placed on the two axles to record the vertical acceleration signal of the unsprung mass. An angular displacement sensor is selected to record the pitch and roll angle of car body. The required feedback states can be obtained through integration of acceleration and differentiation of displacement. A three-dimensional acceleration sensor produced by B & K CO. is placed on driver's seat to calculate weighted root mean square(WRMS). Every seat has a passenger to hold the vehicle's balance. The test car is driven straight down a concrete road with class B surface (ISO8606, 1995) at 40, 60, 80 km/h. The cutoff frequency of the low pass filter is set 50 Hz usually and the sampling frequency is chosen by 200 Hz. Every time the acquired data is divided into 25 sections, and each section has 1024 point. Power spectrum density(PSD) of each sampling data is calculated by 1024-point FFT with an average of 25 sections.

For comparison purposes, the well known sky-hook controller is also formulated and tested. The results are shown in Figs.7,8. For brevity, only the PSD of vehicle body heave is given in Fig.7; other WRMS indexes of acceleration are given in Fig.8. From the Fig.7, it is clearly observed that the vibration of vehicle body between 1 and 10 Hz is significantly reduced using two control strategies compared to passive suspension system. The control performance of skyhook control is inferior to the HSIC in the frequency range of 4 and 8 Hz; the vibration of the frequency range has significant effect on human body. It can also be seen that the WRMS acceleration of the sprung mass is greatly reduced by using HSIC. Simultaneously, the vibration of unsprung mass of semi-active suspension with HSIC has been reduced compared to passive one. However, the semi-active suspension with sky-hook control will degrade the vibration of unsprung mass. It can be concluded that the MR suspension with HSIC can achieve much more improvement in ride comfort and stability than that with skyhook control.

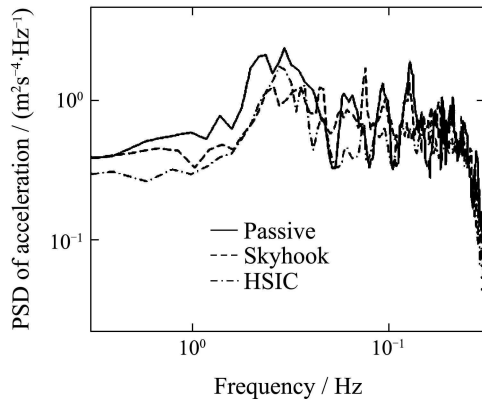


Fig. 7 PSD of comfort pad acceleration at 40 km/h

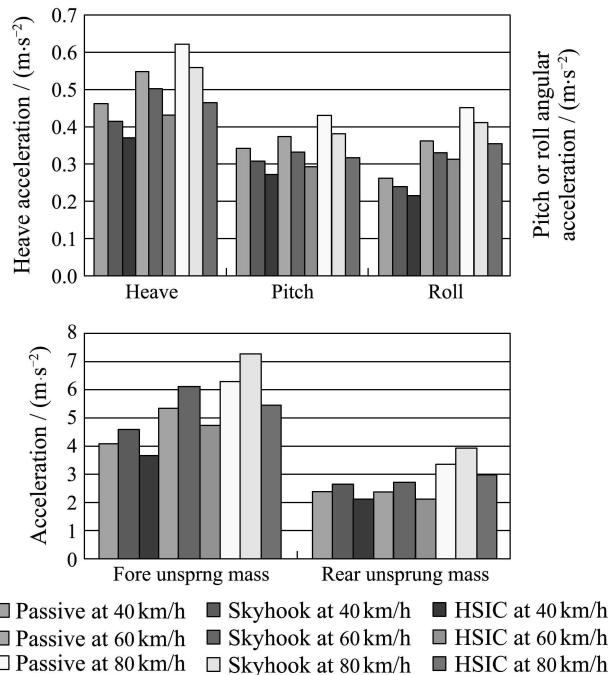


Fig. 8 The vibration acceleration comparison of fore or rear suspension spring and unsprung mass on B class road

5 Conclusion

In this study, an improved human simulated intelligent control(HSIC) based on sensory-motor intelligent schema(SMIS) is proposed to control a magnetorheological(MR) intelligent suspension with significant nonlinearity, time delay and uncertainty. The general design method of HSIC based on SMIS is firstly presented. Then a full vehicle MR suspension model with nonlinearity and time delay is developed. On the basis of the full vehicle mode, a HISC controller based on SMIS is developed. The results of the actual road tests show that HSIC can avoid the ef-

fect of nonlinearity and time-delay of MR dampers, achieve good ride comfort, and restrain pitch and roll motion without reducing the stability. Control performance of HSIC is better than that of independent skyhook control for MR suspension. The successful practice in MR suspension system has also verified the promising future of the HSIC theory based on SMIS that aims at learning and emulating the human “motor sensory preview intelligence” in those control fields with significant nonlinearity, time delay and uncertainty.

参考文献(References):

- [1] MUHAMMAD A, YAO X L, DENG Z C. Review of magnetorheological (MR) fluids and its applications in vibration control[J]. *Journal of Marine Science and Application*, 2006, 5(3): 17 – 29.
- [2] YU M, DONG X M, CHOI S B, et al. Human simulated intelligent control of vehicle suspension system with MR dampers[J]. *Journal of Sound and Vibration*, 2008, 319(3/5): 753 – 767.
- [3] DONG X M, YU M, HUANG S L, et al. Research on frequency-shaping sub-optimal control for semi-active suspension[J]. *Journal of System Simulation*, 2006, 18(10): 3183 – 3186.
- [4] GUO D L, HU H Y, YI J Q. Neural network control for a semi-active vehicle suspension with a magnetorheological damper[J]. *Journal of Vibration and Control*, 2004, 10(3): 461 – 471.
- [5] DONG X M, YU M, HUANG S L, et al. Half car magnetorheological suspension system accounting for nonlinearity and time delay[J]. *International Journal of Modern Physics B*, 2005, 19(7/8): 1381 – 1387.
- [6] ZHOU Q J, BAI J K. An intelligent controller of novel design[C] // *Proceedings of Multi-National Instrumentation Conference, Part. 1*. Shanghai: Science Technology Literature Press, 1983: 137 – 149.
- [7] LI Z S, ZHANG H, WEN Y L, et al. Human simulated intelligent control based on sensory-motor intelligent schemas[C] // *Proceedings of the 5th World Congress on Intelligent Control and Automation*. Hangzhou: IEEE, 2004: 2423 – 2427.
- [8] DONG X M. *Human simulated intelligent control of automobile magnetorheological semi-active suspension*[D]. Chongqing: Chongqing University, 2006.

作者简介:

董小岗 (1975—), 男, 博士, 副教授, 目前研究方向为智能结构及智能控制, E-mail: xmdong@cqu.edu.cn;

李祖枢 (1945—), 男, 教授, 主要研究方向为智能控制与智能自动化, E-mail: zushuli@vip.sina.com;

余 森 (1973—), 男, 博士, 教授, 主要研究方向为智能机械结、结构半主动控制, E-mail: yumiao@cqu.edu.cn;

廖昌荣 (1965—), 男, 博士, 教授, 主要研究方向为汽车智能悬架系统研究, E-mail: crliao@cqu.edu.cn;

陈伟民 (1955—), 男, 博士, 教授, 主要研究方向为光纤机敏土建结构, E-mail: wmchen@cqu.edu.cn.